nature portfolio

https://doi.org/10.1038/s41928-022-00819-6

Supplementary information

In-sensor optoelectronic computing using electrostatically doped silicon

In the format provided by the authors and unedited

In-sensor optoelectronic computing using electrostatically doped silicon

Houk Jang[1,2¶], Henry Hinton[1,¶], Woo-Bin Jung[1], Min-Hyun Lee[3], Changhyun Kim[3], Min Park[4], Seoung-Ki Lee[5], Seongjun Park[3,*], Donhee Ham[1,*]

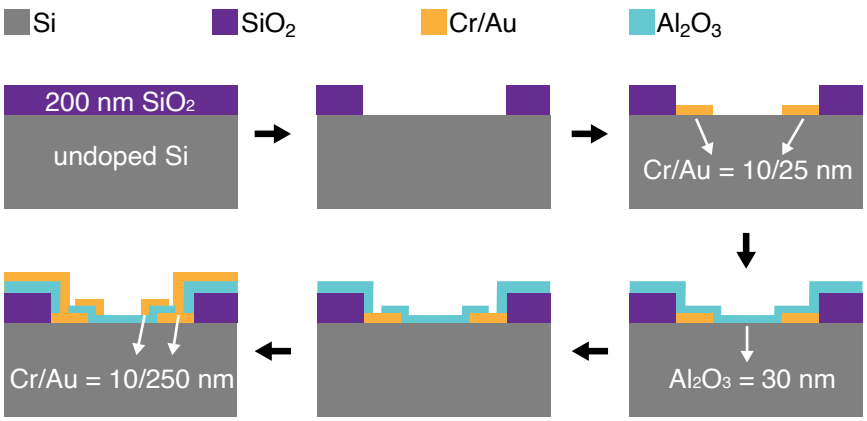

Supplementary Figure 1. Cross-sectional schematic illustration of fabrication steps for the electrostatically doped silicon photodiodes.

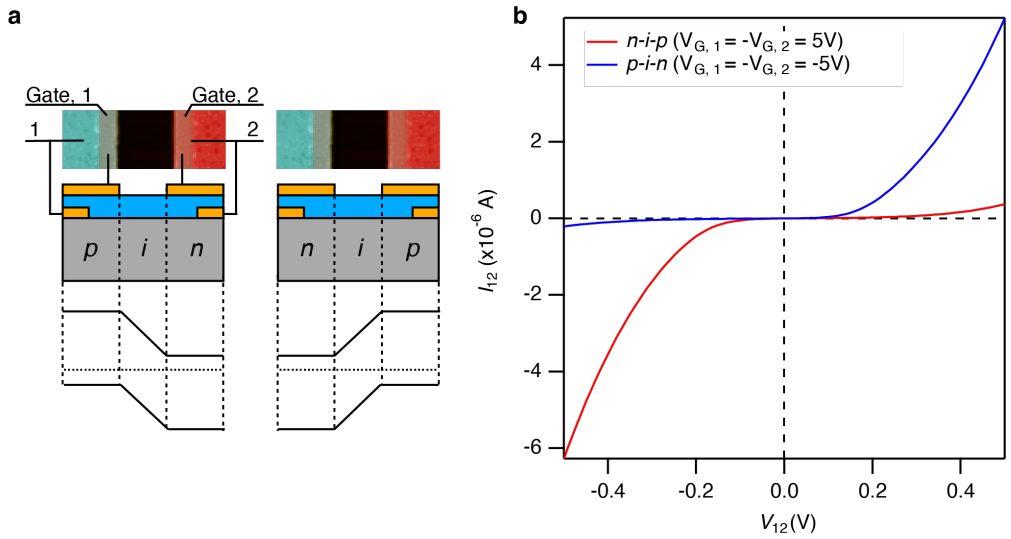

Supplementary Figure 2. Rectifying behavior of the electrostatically doped silicon diode. **a,** False-colored scanning electron microscope (SEM) partial image (top) and corresponding schematic illustration of cross-sectional view of the electrostatically doped diode, biased to form *p-i-n* (left) and *n-i-p* (right) diodes. **b,** The rectifying behavior of the electrostatically formed *p-i-n* (blue) and *n-i-p* (red) diode.

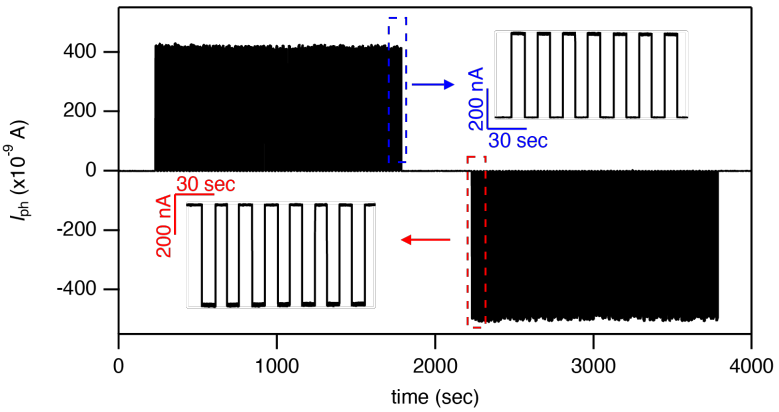

Supplementary Figure 3. Repeated measurement of photocurrent from an electrostatically doped silicon photodiode. The photodiode is biased with V_p (= $V_{G,1}$ = -$V_{G,2}$) of 5 V for 2,000 sec and -5 V for another 2,000 sec and exposed to pulsed light (pulse interval is 20 sec, and pulse width is 10 sec) with a P_{source} of 15 μW (red-filtered halogen lamp).

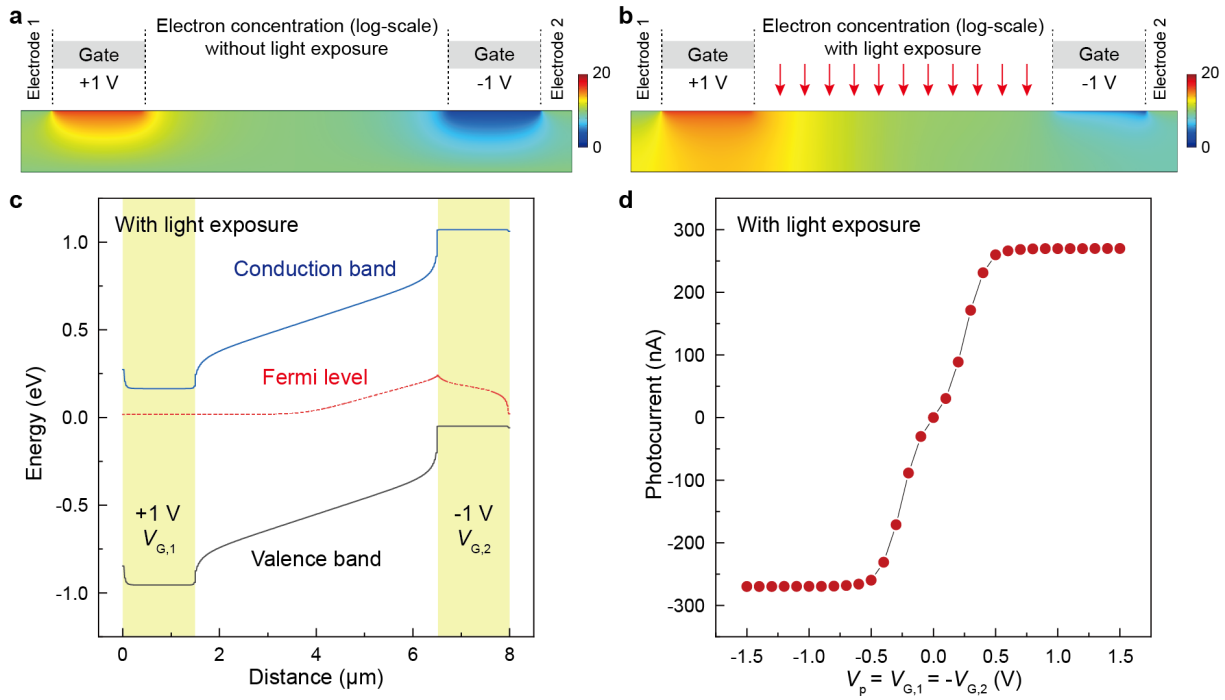

Supplementary Figure 4. COMSOL simulation of the electrostatically doped silicon *p-i-n* diode and its photo response. All contact and gate electrodes are modelled based on the actual device geometry. **a, b,** The profile of electron concentration per cubic meter in the log scale, without and with light illumination (wavelength: 700 nm, incident power per area: 18 W/m^2). $V_{G,1}$ and $V_{G,2}$ are +1 V and -1 V, respectively. **c,** Band diagram with $V_{G,1}$ = 1 V and $V_{G,2}$ = -1 V under light illumination. **d,** photocurrent vs. $V_p = V_{G,1} = -V_{G,2}$.

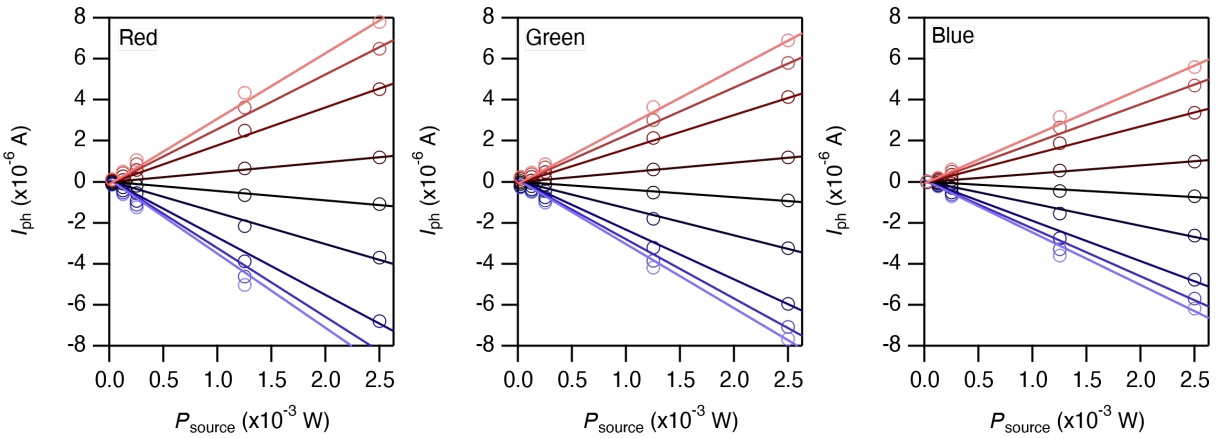

Supplementary Figure 5. Measured photocurrent vs. P_{source}, for red (635 nm), green (520 nm), and blue (473 nm) laser sources.

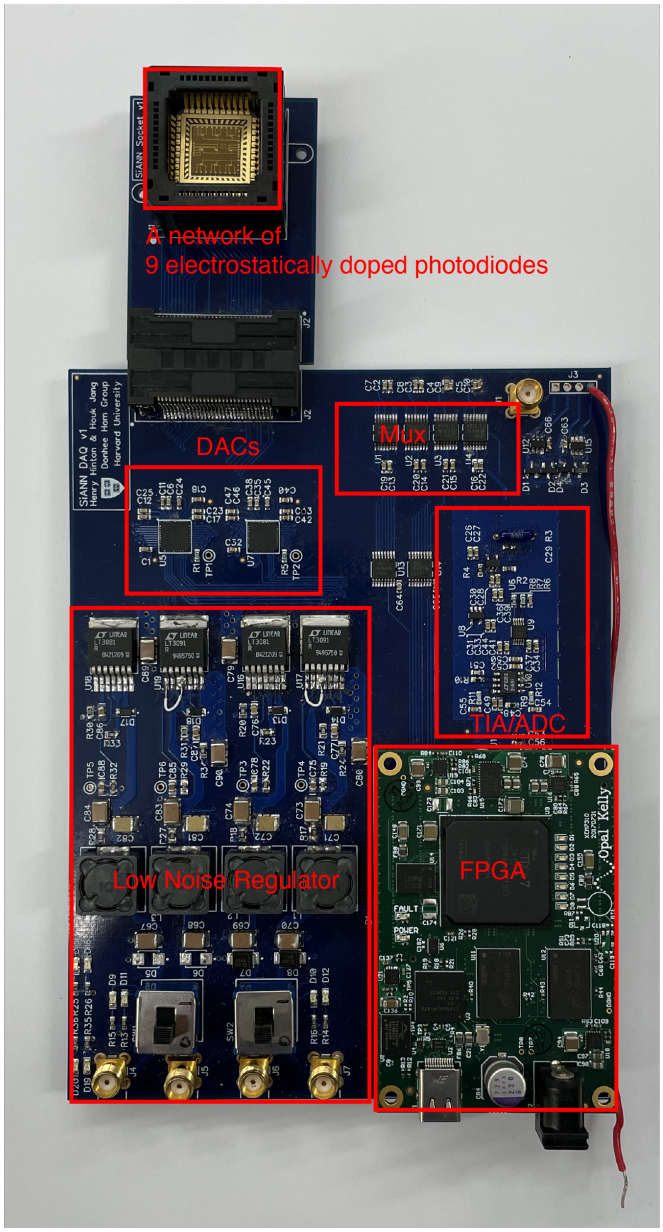

Supplementary Figure 6. Custom printed circuit board (PCB) for the operation of the 9 electrostatically doped silicon photodiode network. The system comprises a low noise regulator, digital-to-analog converters (DACs) for setting gate biases, multiplexers for selecting or combining photocurrents, a transimpedance amplifier (TIA) and an analog-to-digital converter (ADC) for acquiring pA-scale measurements, and an FPGA (Opal Kelly XEM 7310) for aggregating recorded data and communication with the computer.

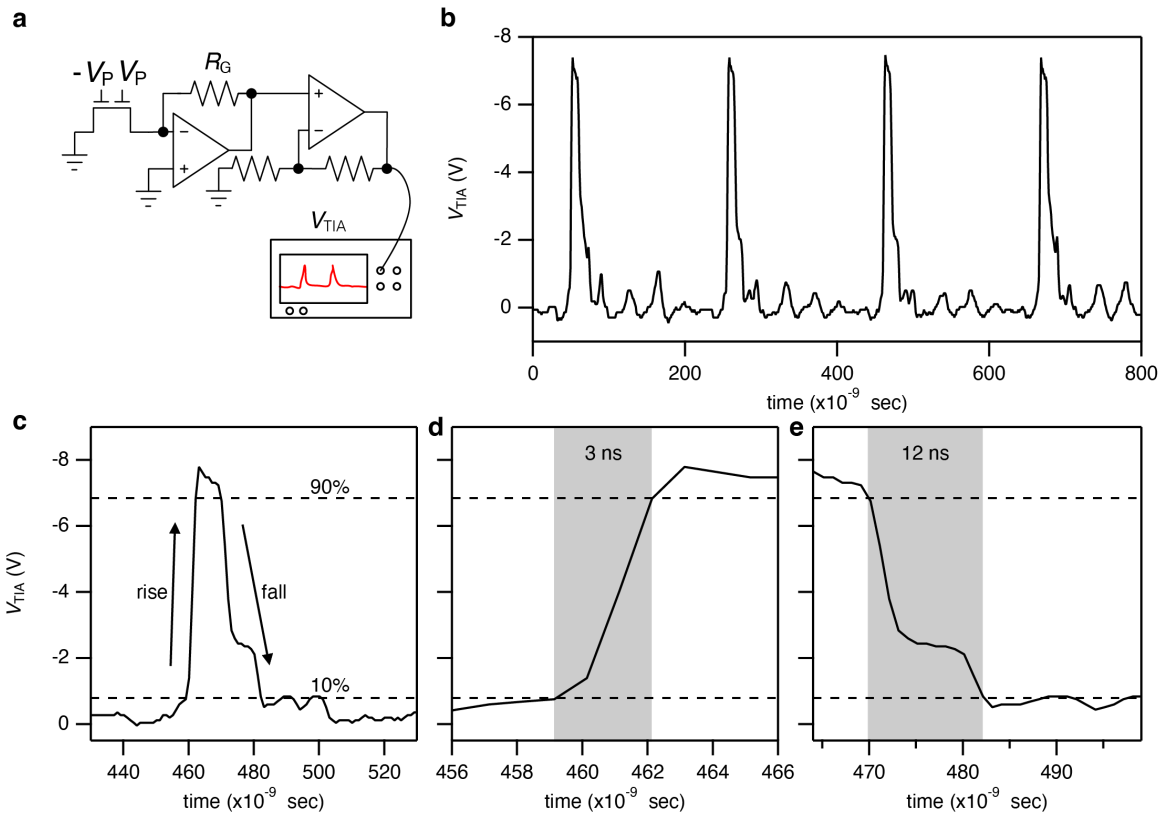

Supplementary Figure 7. Transient photo response of the electrostatically doped diode. **a,** Schematic of the high-speed TIA module—a Texas Instruments OPA858 TIA followed by an extra voltage gain stage—to convert the diode photocurrent to a voltage V_{TIA}. **b,** As the diode with V_p = -2 V is illuminated with a green laser pulse train (NKT SuperK Extreme; pulse width ~5 ps; repetition rate = 5 MHz; average power = 0.81 mW), V_{TIA} measured by a Tektronix MSO 2024B oscilloscope exhibits a voltage pulse train. **c-e,** Rise and fall times of a pulse in this V_{TIA}, measured between 10% and 90% of the full pulse amplitude, are 3 ns and 12 ns. This speed is determined not only by the diode but also by the bandwidth of the TIA module, whose input stage alone has a resistance of 1.5 kΩ and a capacitance of at least 1 pF.

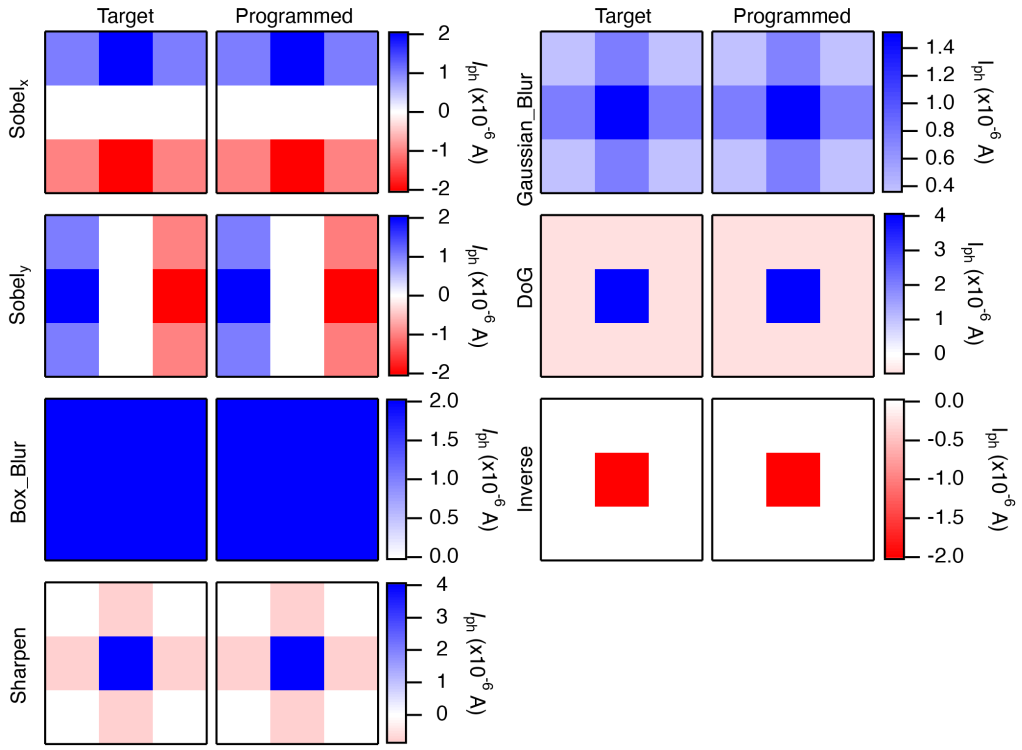

Supplementary Figure 8. Target and programmed photocurrent map for 7 image filter kernels. The color scale at the right side of each programmed map indicates the full range of each filter kernel. An LCD projector (green channel only) whose power is set to 255 out of 255 is used as a light source.

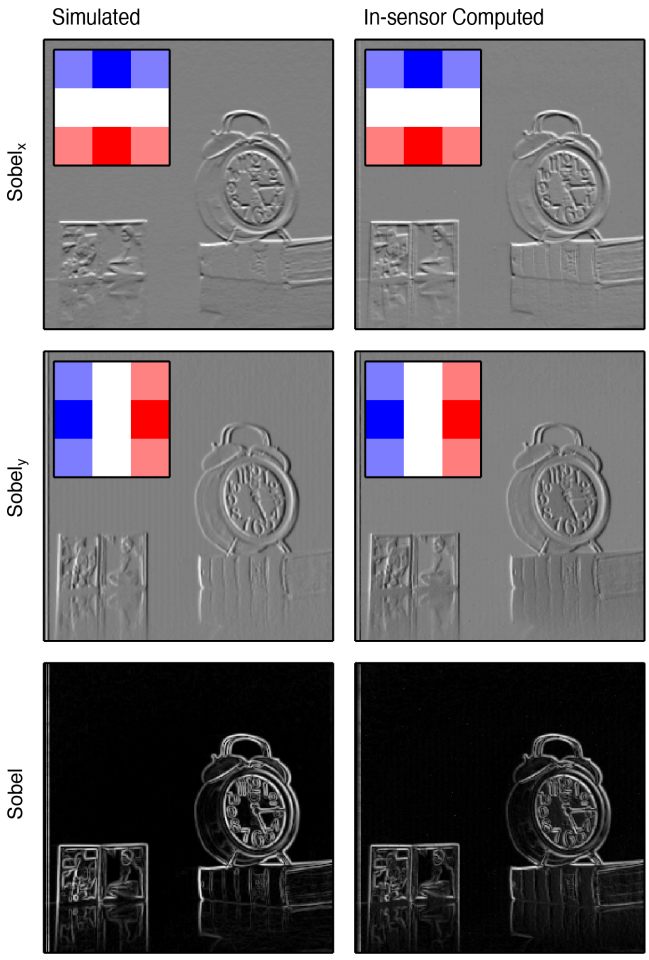

Supplementary Figure 9. Images processed in software (left) and in sensor (right) with vertical (top) and horizontal (middle) Sobel filters. Inset shows the target (left) and programmed (right) filters. The final Sobel filtered images (bottom) are generated by calculating the root sum of squares of each pixel from the horizontal and vertical Sobel filtered images.

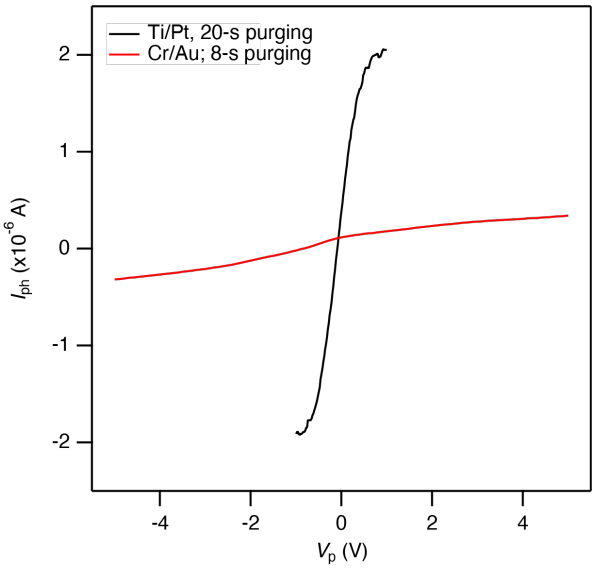

Supplementary Figure 10. Photocurrent vs. V_p for two different electrostatically doped silicon photodiodes, with a red-filtered halogen lamp (P_{source} = 15 μW) as the light source. The red curve is from a diode with Cr/Au contact electrodes and an 8-s purging during the gate dielectric ALD, the same contact electrodes and purging time as used to fabricate all the devices presented in the main text. The black curve is from a diode with Ti/Pt contact electrodes and a 20-s purging. For a given $|V_p|$, the latter device produces a much larger photocurrent than the former device, with the nominal operating range of $|V_p|$ for the latter device reduced below 1 V. This improvement is attributed to the followings. First, Ti/Pt is more compatible to high temperature (250 °C) used for ALD, while Cr/Au can partially aggrege at the high temperature. Ti/Pt thus yields a larger contact area and a lower contact resistance. Second, the increased purging time reduces the amount of remnant reactants/oxidants in the gate dielectric. As an important aside, while the Al_2O_3 gate dielectric in our in-house fabricated device is 30-nm thick, a state-of-the-art CMOS technology fabricates high-k gate dielectric with thickness on the order of 1 nm, with which $|V_p|$ can be further substantially reduced to produce given doping densities, and thus a given photocurrent.